RSC Advances

PAPER

View Article Online
View Journal | View Issue

Cite this: *RSC Adv.*, 2017, **7**, 40189

Theoretical studies on the structure and thermochemistry of cyclicparaphenylenediazenes†

Mohamad Akbar Ali *[a] and Mohammad A. Alam *[b]

Cyclicparaphenylenediazenes (CPPDs) have drawn great attention due to their potential applications in molecular electronics and solar energy. However, to date, there have been no detailed structure and thermochemistry investigations on CPPDs. Herein, we used an integrated computational approach aimed at providing reliable structural and thermochemical information on novel CPPDs based photoswitchable molecular rings. The approach involves hybrid density functional theory calculation at the B3LYP/6-31+G(d,p) level coupled with homodesmotic reaction approach to calculate strain energies (SE) and standard enthalpies of formation ($\Delta_f H^\circ_{298}$) of all *cis* and all *trans* isomers of [*n*]CPPDs (*n* = 2 to 8). The results show that strain energies and $\Delta_f H^\circ_{298}$ per-unit monomer of all *cis*-[*n*]CPPDs (*n* = 4 to 8) increase with increasing the numbers of Ph–N=N linkages. However, an opposite trend was observed for all *trans*-[*n*]CPPDs (*n* = 4 to 8). The results were also compared with carbon nanoring structures *i.e.*, cyclicparaphenyleneacetylenes (CPPAs) and cycloparaphenylenes (CPPs). The calculated highest occupied molecular orbital (HOMO) to the lowest unoccupied molecular orbital (LUMO) energy gaps are in the range of 1.98 eV to 2.36 eV, indicating potential material for the construction of solar cells. The reported structures, SE, $\Delta_f H^\circ_{298}$, and electronic properties of CPPDs can be also helpful to synthesize these novel materials.

Received 8th June 2017
Accepted 8th August 2017

DOI: 10.1039/c7ra06409h

rsc.li/rsc-advances

1. Introduction

Nitrogen-doped cyclic oligomers including cyclic azobenzenophanes (CABPs) have received great attention[1,2] due to their potential applications in semiconductor devices,[3] high-performance catalytic reactions,[4,5] Li-ion batteries,[6] ultracapacitors, optomechanical devices,[7–9] biochemical applications,[10] photoswitches in photopharmacology,[11–13] and molecular motors in drug delivery.[14,15] These attractive properties of CABPs are all due to their *cis–trans* photo and thermal isomerization, and due to their molecular strain.[16–19]

CABPs, in which two, three, and four azobenzene (AB) units are connected by $-CH_2-CH_2-$ and $-CH_2-S-CH_2-$ chains at the *meta* and *para* positions have been studied by various research groups.[16,17] Nagamani *et al.*[17] have reported CABPs, in which two AB are connected by $-CH_2-CH_2-$ group at the *para* positions. They suggested *trans*, *trans* (t,t) isomers are more stable than the *trans*, *cis* (t,c) and *cis*, *cis* (c,c) isomers. In another study, Rau and Lueddecke[18] have prepared an azobenzenophane (ABP), in which two AB are connected by $-CH_2-S-CH_2-$ chains at the *para* positions. They found photoisomerization of ABP was based on a rotation/inversion mechanism from the state of AB, which was inhibited due to the ring strain. In 2013, Durgun and Grossman[19] performed the density functional theory (DFT) calculations on the structure and enthalpies of reaction of *cis* and *trans*-[*n*]azobenzenophanes (*n* = 2 to 6). In their study, the effect of steric distortion on photoisomerization and thermal stability [*n*] azobenzenophanes (*n* = 2 to 6)[19] with $-CH_2-$ linkage were calculated. These CABPs has been suggested for the construction of solar thermal fuel,[20] and photoswitchable devices.[12,13]

The next challenging target in the research field is another important class of CABPs, so called cyclicparaphenylenediazenes (CPPDs). CPPDs are obtained by connecting phenyldiazene (Ph–N=N–) unit through *para* linkage as shown in Fig. 1. CPPDs can be constructed by replacing acetylenic bond (–C≡C–) with an azo group (–N=N–) on cyclicparaphenyleneacetylenes (CPPAs) oligomer[21,22] and can be formed by inserting an azo group between two benzene rings of cycloparaphenylenes (CPPs)[23–25] (Fig. 1). Very few theoretical studies have been carried out on CPPDs.[19,26] As far as we know Durgun and Grossman reported the structure and enthalpies of all *cis* and all *trans* isomer of cyclic[6]paraphenylenediazenes ([6]CPPD).[19] Recently, Van Raden *et al.*[27] have synthesized highly strained nitrogen-doped cyclicparaphenylenes *i.e.*, aza[6]CPP. They calculated highest occupied molecular orbital (HOMO) and lowest unoccupied molecular orbital (LUMO) energy gap

[a]*Department of Chemistry, Sejong University, Seoul, 143-747, Republic of Korea. E-mail: akbar256@sejong.ac.kr*

[b]*Department of Chemistry and Physics, College of Science and Mathematics, Arkansas State University, Jonesboro, AR 72467, USA. E-mail: malam@astate.edu*

† Electronic supplementary information (ESI) available: Tables of optimized geometries, vibrational frequencies, ZPEs, thermal correction, entropy for CPPDs. Table of ring diameter of CPPDs, CPPAs, and CPPs and figures showing HOMO, LUMO and HOMO–LUMO gap of CPPDs. See DOI: 10.1039/c7ra06409h

level using hybrid DFT at B3LYP/6-31G(d) level. In another study, Yuan *et al.*[26] have predicted the host–guest interaction between [6]CPPD and [7]CPPD with fullerene (C_{60}) using hybrid DFT at M06-L and M06-2X levels. They reported the relative stabilities of host–guest interactions between fullerene C_{60} and [6]CPPD and [7]CPPD by varying nitrogen atoms in the ring.

Over the years, many hypothetical chemical reactions have been proposed in an effort to predict the thermochemistry of organic and inorganic molecules. Since Baeyer's[28] classic strain theory from 1885 and Bredt's rule almost 100 years ago, strained hydrocarbons have aroused considerable interest to chemists and material scientists. Efforts of chemists to bend and break Bredt's rule have generated a great variety of interesting molecules. Angle strained cyclic oligomer *i.e.*, CPPAs, CPPs, and CPPDs are the important class of strained hydrocarbons that are attractive to both experimental and theoretical chemists.[19,22,25] Some of these molecules are useful in photovoltaic cells because they have strong electron withdrawing character of the triple bond and their rod-like structure.[29]

The group equivalent method, Westheimer bond angle method,[30] Dudev ring fragment method,[31] Wiberg heats of reaction method, isodesmic,[32–37] connectivity-based hierarchy,[38] and homodesmotic reaction approaches, *etc.*,[21,32,39–41] are a few widely used methods in literature for calculating strain energies (SE) and standard enthalpies of formation ($\Delta_f H^\circ_{298}$) of cyclic and acyclic molecules. In this paper, we have used similar approaches *i.e.*, isodesmic and homodesmotic reaction schemes coupled with density functional theory to analyze the trends of SE and $\Delta_f H^\circ_{298}$ of CPPDs.

To the best of our knowledge, there have been no experimental and theoretical studies on structure, thermochemistry, and electronic properties of all *cis* and all *trans* isomers of cyclic [*n*]paraphenylenediazenes ([*n*]CPPDs) ($n = 2$ to 8). The synthesis of angle-strained [*n*]CPPDs is highly desirable due to their potential application in π-conjugated organic materials. In this paper we attempt to quantify this synthetic challenge, by applying an integrated computational strategy aimed at providing reliable structure, molecular orbitals, SE, and $\Delta_f H^\circ_{298}$ for all *cis* and all *trans*-CPPDs. The SE of highly strained CPPDs and weakly strained CPPDs molecules have a significant impact on their stability and reactivity, were calculated using hybrid density functional methods in combination of homodesmotic reaction approach.[39] The SE of CPPDs was also compared with its analogous π-conjugated oligomer (Fig. 1) *i.e.*, CPPs and CPPAs, which have been suggested for the model compounds for carbon nanotube and carbon nanobelt.[21,22,25,40] To further explore the structure of novel CPPDs and its applications in molecular electronics and in solar energy, we calculated the energies of HOMO, LUMO, and HOMO–LUMO gap.

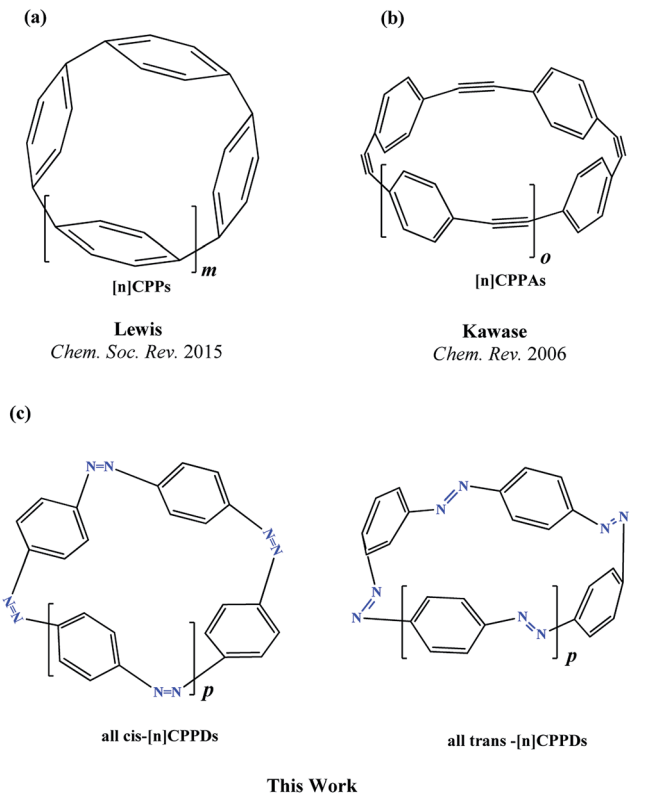

Fig. 1 Structure of (a) [*n*]CPPs, where *m* ($m = n - 3$) represents phenyl (Ph–) monomer (b) [*n*]CPPAs, where *o* ($o = n - 3$) represents Ph–C≡C– monomer and (c) [*n*]CPPDs,, where *p* ($p = n - 3$) represents number of Ph–N=N monomer. The all *cis* isomers of CPPDs are represented as [2_c]CPPD, [3_c]CPPD, [4_c]CPPD, [5_c]CPPD, [6_c]CPPD, [7_c]CPPD, and [8_c]CPPD and all *trans* isomers of CPPDs are represented as [2_t]CPPD, [3_t]CPPD [4_t]CPPD, [5_t]CPPD, [6_t]CPPD, [7_t]CPPD, and [8_t]CPPD.

2. Theoretical methodology

The geometrical, energetical, vibrational, and electronic properties of all *cis*-[*n*]CPPDs (designated as [n_c]CPPDs) ($n = 2$ to 8) and all *trans*-[*n*]CPPDs isomer of [*n*]CPPDs (designated as [n_t]CPPDs) ($n = 2$ to 8) were performed using hybrid DFT; B3LYP[42] in conjunction with 6-31+G(d,p) basis set as implemented in the Gaussian 09 (Rev. D.01) and Gaussian 09 (Rev.E.01) program suites.[43,44] No symmetry constraint was applied during geometry optimization. Optimized geometries and vibrational frequencies are tabulated in the ESI (Tables S1–S4†). The nature of all stationary points on the potential energy surface (PES) (minimum) was checked by diagonalizing the corresponding Hessians. The absence of imaginary frequency confirms that the obtained structure corresponds to a true minimum on the potential energy surface. The zero-point energy (ZPE), and thermal correction (ΔH_T) were calculated from vibrational frequency analysis. We have chosen the B3LYP model, since it produces reasonably good π-conjugated structures, and appropriate for the prediction of electronic structure of polycyclic hydrocarbons and their energies.[21,27,34,35,40,45–48] The combination of B3LYP[42] with 6-31G(d) and 6-31+G(d,p) basis sets has been tested by other groups and results were found to be in good agreement with experimental values.[21,40,46,48] Therefore, we believe the same combination will provide reasonably accurate geometrical parameters and vibrational frequencies for [*n*]CPPDs.

Some calculations were also carried out using high-level quantum composite Gaussian-4 (G4) method[49] as implemented in the Gaussian 09 (Rev. D.01)[43] and Gaussian 09

(Rev.E.01)[44] program suites. The G4 theory[49] is the fourth in the Gaussian-*n* series of quantum chemical methods, which is based on geometry optimization as well vibrational analysis of molecules at the B3LYP/6-31G(2df,p). This calculation is followed by a series of single-point energy calculations with higher level of theory: CCSD(T,FC)/6-31G(d), MP4 (FC)/6-31G(d), MP4(FC)/6-31+G(d), MP4 (FC)/6-31G(2df,p), and MP2(FU)/G3LargeXP.[49] The G4 method produces approximate energy accuracy of ±1 kcal mol^{-1}.[49]

The calculation of SE and $\Delta_f H^\circ_{298}$ of [*n*]CPPDs were carried out using similar homodesmotic reaction approach[39] as discussed in previous works.[21,24] The SE and $\Delta_f H^\circ_{298}$ of a hypothetical isodesmic or homodesmotic reaction schemes of unknown molecule A of reaction type $n\mathrm{A} + m\mathrm{B} \rightarrow r\mathrm{C} + s\mathrm{D}$ were calculated using;

$$\text{Strain energy} = \sum \Delta E^{\text{products}}_{0\ \mathrm{K}} - \sum \Delta E^{\text{reactants}}_{0\ \mathrm{K}} \quad (1)$$

where, $\Delta E^{\text{products}}_{0\ \mathrm{K}}$ and $\Delta E^{\text{reactants}}_{0\ \mathrm{K}}$ are the energy differences for products and reactants at 0 K.

$$n\Delta_f H^\circ_{298}(\mathrm{A}) = r\Delta_f H^\circ_{298}(\mathrm{C}) + s\Delta_f H^\circ_{298}(\mathrm{D}) - m\Delta_f H^\circ_{298}(\mathrm{B}) - \Delta H^{\text{rxn}}_{298} \quad (2)$$

where, $\Delta_f H^\circ_{298}$ (B), $\Delta_f H^\circ_{298}$ (C), and $\Delta_f H^\circ_{298}$(D) are enthalpies of formation of species B, C, and D, respectively and $\Delta H^{\text{rxn}}_{298}$ is the enthalpies of reaction for reaction $n\mathrm{A} + m\mathrm{B} \rightarrow r\mathrm{C} + s\mathrm{D}$.

All the optimized geometrical parameters and vibrational frequencies are given in the ESI.† Strain energies, enthalpies of reaction, enthalpies of formation, and enthalpies of combustion are expressed in kJ mol^{-1}, vibrational frequencies in cm^{-1} and HOMO, LUMO, and HOMO–LUMO gap energies in eV.

3. Results and discussion

3.1 Structure of [*n*]CPPDs

Before discussing thermochemistry and electronic properties, it is necessary to examine the molecular geometries of CPPDs, since they are closely related to physical and chemical properties. Structure of all *cis*-[n_c]CPPDs (n = 2 to 8) and all *trans*-[n_t]CPPDs (n = 2 to 8) were optimized using at B3LYP/6-31+G(d,p) level of theory. Optimized structures of all *cis* and all *trans*-CPPDs are shown in Fig. 2 and 3, respectively. To find out the different conformations of all *trans*-CPPDs and all *cis*-CPPDs, we have carried out many geometry optimizations. For example, in the case of all *trans*-[6_t]CPPD, we started different orientation of phenyl group in [6_t]CPPD and in all cases, we have obtained a stable circular structure as shown in the ESI Fig. S1.† Therefore, we believe that the possibilities of other stable structures are negligible for all *trans*-CPPDs. However, in case of all-*cis* CPPDs, we have found the different conformation of [6_c]CPPD, [7_c]CPPD, and [8_c]CPPD as shown in the Fig. 2. The mix

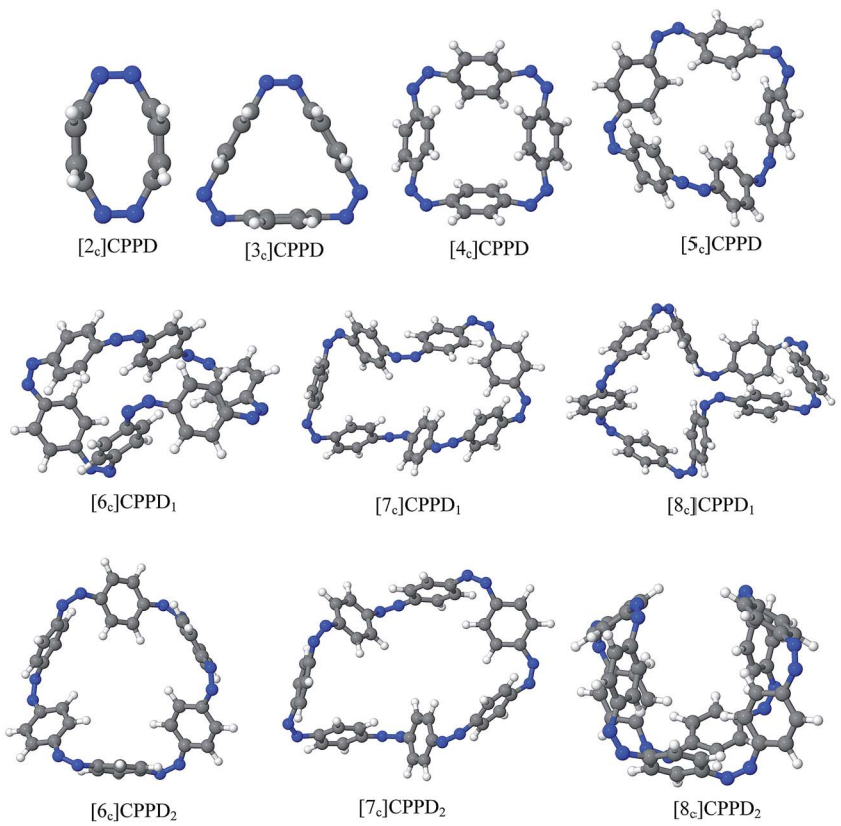

Fig. 2 Optimized structures of all *cis*-[*n*]CPPDs (n = 2 to 8) obtained using B3LYP/6-31+G(d,p) level of theory. The hydrogen, carbon, and nitrogen atoms are indicated by white, grey, and blue spheres, respectively. The different conformation of [6_c]CPPD, [7_c]CPPD and [8_c]CPPD are represented using 1 and 2.

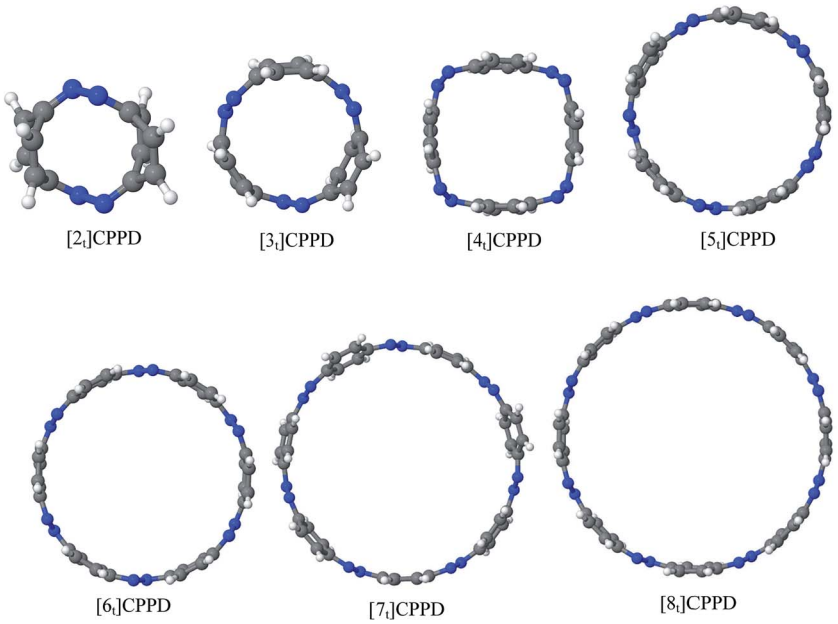

Fig. 3 Optimized structure of *trans*-[*n*]CPPDs (n = 2 to 8) obtained using B3LYP/6-31+G(d,p) level of theory. The hydrogen, carbon, and nitrogen atoms are indicated by white, grey, and blue spheres, respectively.

combination of *cis* and *trans* isomers may be important and but is not the focused of the current study. In previous reports, researchers have shown the importance all *cis* and *trans* isomers of CPPDs.[19,26] For example; Durgun and Grossman have shown the photoisomerization of all *cis* and all *trans* isomers of OH-substituted 3-azobenzenophanes and 4-AB azobenzenophanes.[19] In another study, Yuan *et al.*[26] have predicted the host–guest interaction between only all *trans*-[6]CPPD and all-*trans*-[7]CPPD with fullerene (C_{60}). In the present study, we focused only on all *cis* and all *trans* form of [*n*]CPPDs, but in future, we plan to examine combination of *cis* and *trans* isomers of [*n*]CPPDs.

ESI Table S5† lists some selected bond lengths and bond angles of [n_c]CPPDs (n = 2 to 8) and [n_t]CPPDs (n = 2 to 8) at the B3LYP/6-31+G(d,p). This table also includes the calculated bond lengths and bond angles of reference compounds *i.e.*, *cis* and *trans* 1,4-bis(diazenyl)benzene (bDB), and *cis* and *trans* azobenzene (AB) and experimentally reported value for AB.[50] The C–N and N=N bond distance and bond angle in [2_c]CPPD and [3_c]CPPD are quantitatively similar to bDB and AB. These values are in very good agreement with reported experimental values.[50] The CNNC angles of [2_t]CPPD (~85.6°), [3_t]CPPD (104.9°) and [4_t]CPPD (134.9°) are smaller than strain free bDB and *trans* AB (~180°). The higher deviation of angle shows maximum angle strain in the *trans* CPPDs series (Table S5†). As shown in the Table S5,† large bond distortion and dihedral angle of [2_t]CPPD, [3_t]CPPD, and [4_t]CPPD may destabilize the structures through maximizing the molecular strain energy. The C–N and N=N bond lengths and C–N=N bond angle of *cis*-[4_c]CPPD are different from its *trans*-[4_t]CPPD isomers. This is due to the fact that *cis* isomer was found to be a stable boat form and *trans* isomer was found as a ring type structure (Fig. 2 and 3). The bond length and bond angle of higher members show a little variation compared to those *cis–trans* bDBs and *cis–trans* ABs. The dihedral angle of *trans*-[*n*]CPPDs (n = 4 to 8) approaches ~180° as the number of n increases, which may stabilize the structures. The calculated values of *cis* and *trans* isomers of AB are also in very good agreement with reported experimental

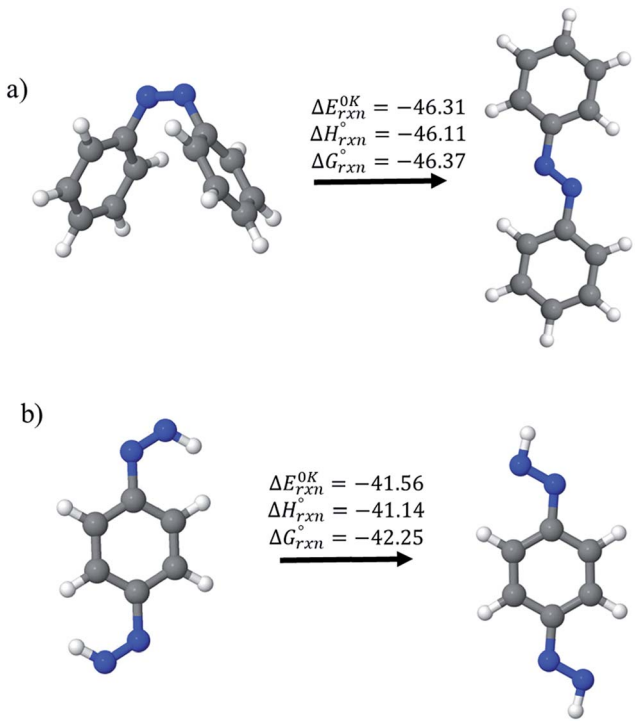

Fig. 4 Enthalpies of reaction (at 0 K and 298 K) and Gibbs free energies (at 298 K) of *cis* → *trans* isomerization of (a) azobenzene and (b) 1,4-bis(diazenyl)benzene computed using G4 method.

values.[50] The point group symmetry of [*n*]CPPDs ($n = 2$ to 8) has been listed in Table S5.† The point group symmetry of [2_c]CPPD is D_{2h} which is similar to the point group symmetry of highly strained cyclic[2]paraphenyleneacetylenes ([2]CPPA) in the [*n*] CPPAs series. However, the point group symmetry of [2_t]CPPD is C_{2h}. The point group symmetry of [3_c]CPPD (C_s) and [3_t]CPPD (C_2) is different from [3]CPPA (D_{3h}). The generalized point group for the higher member of *trans*-[*n*]CPPDs ($n > 3$) is D_n. The point group of all *cis* isomers varies as *n* increases (Table S5†). The predicted point group symmetry of *cis* and *trans* isomers of CPPDs are different from its analogous oligomer *i.e.*, cyclic-paraphenyleneacetylenes (CPPAs) and cycloparaphenylenes (CPPs).[21–24]

3.2 Reaction energies

Before considering ring systems, we first calculated ΔE (at 0 K), ΔH (at 298 K), and ΔG (at 298 K) for the *cis* → *trans* photo isomerization of open azobenzene (AB) and 1,4-bis(diazenyl) benzene (bDB) using G4 method (Fig. 4). The *trans* isomer of AB is found to be more stable than *cis* isomer of AB by ~46.1 kJ mol^{-1}, which is in good agreement with reported experimental value (48.5 kJ mol^{-1}). The G4 enthalpy (46.1 kJ mol^{-1}) were also compared with theoretically calculated value (55.9 kJ mol^{-1}) by Durgun and Grossmann.[19] Their calculated value (8–9 kJ mol^{-1}) using hybrid DFT functional is higher than that of our calculated value (46.1 kJ mol^{-1}) and experimentally reported one (48.5 kJ mol^{-1}). In case of bDB, *cis* → *trans* photo isomerization is (~41 kJ mol^{-1}), this value is ~5 kJ mol^{-1} lower than AB.

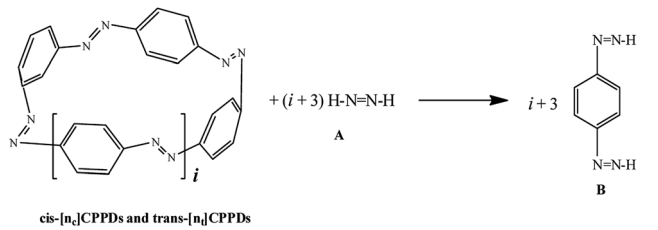

Scheme 1 Hypothetical homodesmotic reactions for the calculation of strain energies of [*n*]CPPDs.

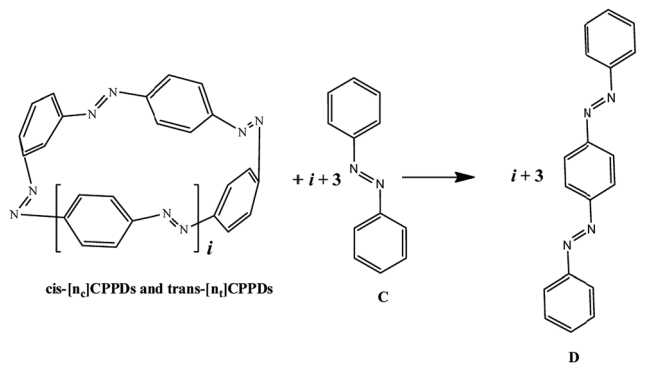

Scheme 2 Hypothetical homodesmotic reactions for the calculation of strain energies of [*n*]CPPDs.

AB has most often served as a model system for the study of N=N based *cis* and *trans* isomerization in CPPDs, because it absorbs light and experimentally convenient to study. Therefore, we believe that CPPDs, which contain 2 to 7 azobenzene units have been of interest in studying the steric distortion on the photochemical *cis* and *trans* isomerization. Because strain-free oligomers of CPPDs have not been reported so far, we have applied two different hypothetical homodesmotic reaction Scheme 1 (based on Ali and Krishnan study),[21] and Scheme 2 (based on Segwa *et al.*),[24] to calculate the strain energies (SE) of CPPDs. $\Delta_{rxn}H^{\circ}_{298}$ calculated using both schemes are shown in Fig. 5 and tabulated in Table 1. The $\Delta_{rxn}H^{\circ}_{298}$ of both schemes is lower for smaller members and increases as the number of Ph–N=N linkages increase. The bar diagram (Fig. 5) shows that $\Delta_{rxn}H^{\circ}_{298}$ of Scheme 1 is lower than Scheme 2, indicating HD Scheme 1 has less error compared to HD Scheme 2.

The SE at 0 K (*i.e.*, with the zero-point correction included) for the all *cis* and all *trans* isomer of [*n*]CPPDs ($n = 2$ to 8) were calculated using both schemes are listed in Table 1. The difference in SE using Schemes 1 and 2 for lower members are smaller. However, for the higher member of CPPDs these values are larger. The SE of [2_c]CPPD and [2_t]CPPD has the highest SE in [n_c]CPPDs ($n < 5$) series, and [n_t]CPPD series, respectively. This is mostly due to its distorted sp^2–sp^2–sp^2 angle (117.2°) in [2_c]CPPD and (85.6°) [2_t]CPPD. The SE of [n_c]CPPDs ($n = 5$ to 8) is higher than all *trans*-[n_t]CPPDs ($n = 5$ to 8), which may be attributed to the higher dihedral angle of *cis* isomer than that of *trans* isomer (Table S5†). The SE of all *cis* isomer increases linearly with adding each Ph–N=N unit. The SE of *trans* isomer decreases linearly with increasing Ph–N=N unit. The higher SE of [8_c]CPPD, [7_c]CPPD, [2_t]CPPD, [6_c]CPPD, [2_c]CPPD, [3_t]CPPD, [4_t]CPPD, and [5_c]CPPD may not favour their synthesis. However, the lower SE of [4_c]CPPD, [3_c]CPPD, [5_t]CPPD, [6_t] CPPD, [7_t]CPPD, and [8_t]CPPD may favour the synthesis of these molecules.

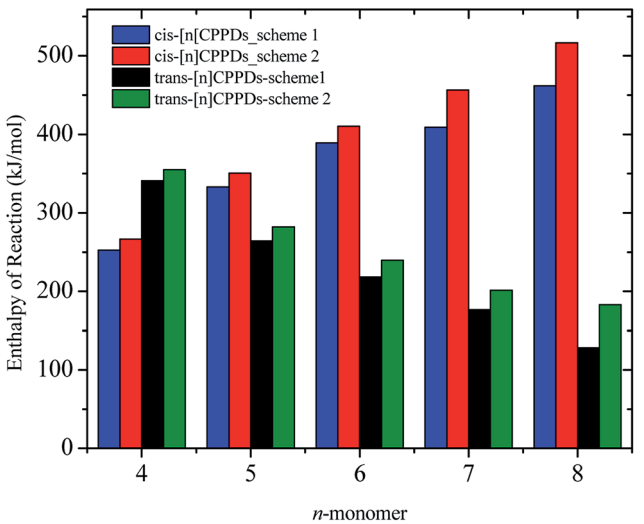

Fig. 5 Enthalpies of reaction calculated using Schemes 1 and 2. Only stable conformation of all *cis* of [n_c]CPPDs ($n = 6$ to 8) are shown.

Table 1 ΔH^{rxn}_{298} (kJ mol^{-1}) and SE (kJ mol^{-1}) calculated based on homodesmotic Schemes 1 and 2 using at B3LYP/6-31+G(d,p) level

Homodesmotic reaction schemes					
All-*cis* CPPDs	ΔH^{rxn}_{298}	SE	All-*trans* CPPDs	ΔH^{rxn}_{298}	SE
[2_c]CPPD + 2A → 2B^a	−353.3	*351.5*	[2_t]CPPD + 2A → 2B^a	−403.3	401.8
[2_c]CPPD + 2C → 2D^b	*−360.4*	*364.6*	*[2_t]CPPD + 2C → 2D^b*	−410.5	414.9
[3_c]CPPD + 3A → 3B^a	−230.6	226.3	[3_t]CPPD + 3A → 3B^a	−299.4	295.7
[3_c]CPPD + 3C → 3D^b	*−241.3*	*246.0*	*[3_t]CPPD + 3C → 3D^b*	−310.1	315.4
[4_c]CPPD + 4A → 4B^a	−252.5	245.8	[4_t]CPPD + 4A → 4B^a	−340.9	334.7
[4_c]CPPD + 4C → 4D^b	*−266.8*	*272.0*	*[4_t]CPPD + 4C → 4D^b*	*−355.2*	*361.0*
[5_c]CPPD + 5A → 5B^a	−332.7	323.3	[5_t]CPPD + 5A → 5B^a	−264.5	255.6
[5_c]CPPD + 5C → 5D^b	*−350.5*	*356.0*	*[5_t]CPPD + 5C → 5D^b*	*−282.3*	*288.4*
^{1}[6_c]CPPD$_1$ + 6A → 6B^a	−401.0	388.9	[6_t]CPPD + 6A → 6B^a	−218.5	206.4
^{2}[6_c]CPPD$_2$ + 6A → 6B^a	−389.0	377.1			
^{1}[6_c]CPPD$_1$ + 6C → 6D^b	*−422.4*	*428.2*	*[6_t]CPPD + 6C → 6D^b*	*−239.9*	*245.7*
^{2}[6_c]CPPD$_2$ + 6C → 6D^b	−410.4	416.5			
^{1}[7_c]CPPD$_1$ + 7A → 7B^a	−408.9	394.1	[7_t]CPPD + 7A → 7B^b	−176.5	161.8
^{2}[7_c]CPPD$_2$ + 7A → 7B^a	−420.6	405.5			
^{1}[7_c]CPPD$_1$ + 7C → 7D^a	*−456.6*	*679.1*	*[7_t]CPPD + 7C → 7D^a*	*−201.4*	*207.7*
^{2}[7_c]CPPD$_2$ + 7C → 7D^a	−468.2	*690.6*			
^{1}[8_c]CPPD$_1$ + 8A → 8B^{a,c}	−463.1	445.7	[8_t]CPPD + 8A → 8B^{b,c}	−128.4	110.0
^{2}[8_c]CPPD$_2$ + 8A → 8B^{a,c}	−462.0	445.6			
^{1}[8_c]CPPD$_1$ + 8C → 8D^{a,c}	*−517.6*	*771.4*	*[8_t]CPPD + 8C → 8D^{a,c}*	*−182.9*	*435.8*
^{2}[8_c]CPPD$_2$ + 8C → 8D^{a,c}	−516.5	771.4			

^{a} ΔH^{rxn}_{298} and SE calculated based on Scheme 1. ^{b} ΔH^{rxn}_{298} and SE calculated based on Scheme 2. ^{c} Calculated using B3LYP/6-31G(d) level. A: HN=NH; B: HN=N–Ph–N=NH; C: Ph–N=N–Ph; D: Ph–N=N–Ph–N=N–Ph; Ph: phenyl ring,[1,2] different conformation of *cis*-CPPD.

Fig. 6 details the thermodynamic stability *i.e.*, enthalpies and Gibbs free energies of [n_c]CPPDs and [n_t]CPPDs (n = 4 to 8) and isolated AB and bDB. Positive values of $\Delta H^{rxn}_{0\ K}$ and $\Delta G^{\circ}_{298\ K}$ indicate all the *cis*-CPPDs is more stable, whereas negative values indicate all *trans*-CPPDs are more stable. In all cases (n = 5 to 8), *trans* isomers are more stable than *cis* isomers, however, for n = 4, *cis* isomer is more stable than the *trans* isomer. This is due to the fact that [4_c]CPPD is less strained compared to [4_t]CPPD (see Fig. 2 and Table S5†). The computed ZPE, thermal correction (H_T), and entropy of all *cis* and all *trans* isomers are in tabulated in the ESI (Table S6†). The ΔZPE, ΔH_T, and ΔS of *cis* → *trans* transformation isomers are very small. The relatively smaller value of ΔS can be explained by assuming that the isomerization of *cis*-CPPDs or *trans*-CPPDs can start from a structure that has the smaller degree of freedom because of the strain caused by a cyclic structure.

The calculated SE of [n]CPPDs (n = 4 to 8) are compared with previously calculated SE of [n]CPPs and [n]CPPAs (n = 4 to 8) as shown in Fig. 7. The SE of [n_t]CPPDs decreases with increasing Ph–N=N units, which is consistent with [n]CPPAs (strain energies decreases linearly as Ph–C≡C) and CPPs (SE decreases

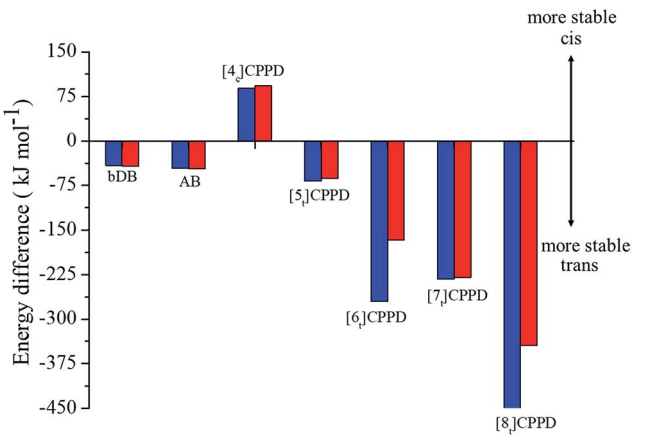

Fig. 6 Enthalpy difference ($\Delta H^{rxn}_{0\ K}$) and Gibbs free energy ($\Delta G^{\circ}_{298\ K}$) change between *cis* and *trans* isomers. Blue line corresponds to $\Delta H^{rxn}_{0\ K}$ and red line corresponds to $\Delta G^{\circ}_{298\ K}$.

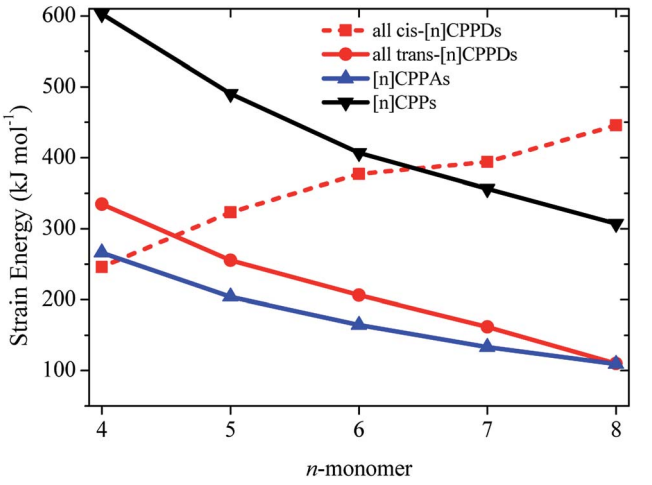

Fig. 7 Comparison of SE calculated using homodesmotic Scheme 1 for [n]CPPDs (n = 4 to 8) and the SE value of [n]CPPAs (n = 4 to 8)[21] and [n]CPPs (n = 4 to 8).[23,24]

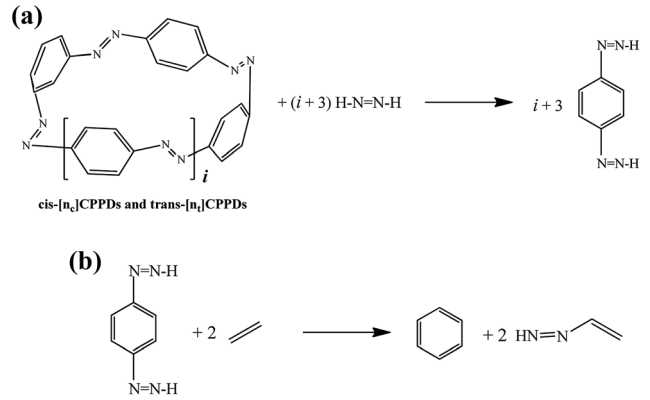

Scheme 3 Hypothetical homodesmotic reactions for the calculation of $\Delta_f H^\circ_{298}$ of all *cis* and all *trans*-[*n*]CPPDs.

linearly as Ph– unit increases). The SE of [4$_c$]CPPD, [5$_c$]CPPD, and [6$_c$]CPPD are lower than that of [4]CPP, [5]CPP, and [6]CPP respectively. The SE value for [7$_c$]CPPD and [8$_c$]CPPD are higher than that of respective [7]CPP and [8]CPP. This effect is due to the twisted structure, which imposes higher dihedral angle in the higher member of CPPDs. If we compare the SE of *trans* isomer of CPPDs with CPPAs and CPPs, the order of SE of these oligomer are [*n*]CPPs > [n_t]CPPDs > [*n*]CPPAs (n = 4 to 7).

SE is a good indicator in the feasibility of synthesis process. Some of the carbon nanoring structure *i.e.*, [5]CPP (490.5 kJ mol^{-1}), [6]CPP (406.8 kJ mol^{-1}), [7]CPP (356.5 kJ mol^{-1}), [8]CPP (307.1 kJ mol^{-1}), [9]CPP (274.5 kJ mol^{-1}), [12]CPP (201.3 kJ mol^{-1}), [18]CPP (132.6 kJ mol^{-1}), [6]CPPA (164.4 kJ mol^{-1}), [7]CPPA (133.3 kJ mol^{-1}), and [8]CPPA (109.4 kJ mol^{-1}) have already been synthesized by various research groups.[22,23,51–53] Therefore, we believe the same synthetic strategies may also be applied for the synthesis of all *cis* and all *trans* isomers of CPPDs with lower SE values.

The standard enthalpies of formation ($\Delta_f H^\circ_{298}$) is a fundamental quantity in the estimation of the energy stored in [*n*] CPPDs (n = 2 to 8). $\Delta_f H^\circ_{298}$ is calculated using the combination of homodesmotic reactions (Schemes 3a and b). The $\Delta_f H^\circ_{298}$ of *cis* and *trans* isomers of CPPDs are shown in Table 2. The experimental $\Delta_f H^\circ_{298}$ of 1,4-bis(diazenyl)benzene (bDB) is unknown. Therefore, our calculation of $\Delta_f H^\circ_{298}$ of bDB is based on another homodesmotic approach (Scheme 3b). The $\Delta_f H^\circ_{298}$ of bDB is calculated using high-level quantum composite Gaussian-4 method.[49] The experimental gas-phase $\Delta_f H^\circ_{298\ K}$ of benzene (82.8 kJ mol^{-1})[54] and ethylene (20.4 kJ mol^{-1}) is used to obtain the value of bDB (522.9 kJ mol^{-1}). However, the experimental $\Delta_f H^\circ_{298\ K}$ of reference HN=NCH=CH$_2$ is not known. Therefore, our calculation of $\Delta_f H^\circ_{298}$ for HN=NCH=CH$_2$ is based on another hypothetical isodesmic reaction (HN=NCH=CH$_2$ + CH$_4$ → H$_3$CN=NH + C$_2$H$_4$). The experimental $\Delta_f H^\circ_{298}$ for CH$_3$N=NH is taken from Matus *et al.* study[55] for the calculation of $\Delta_f H^\circ_{298}$ for HN=NCH=CH$_2$. The calculated $\Delta_f H^\circ_{298}$ of HNNCH=CH$_2$ using isodesmic reaction approach is 266.8 kJ mol^{-1}. The $\Delta_f H^\circ_{298}$ per-unit monomer of all *cis* and all *trans* isomers of [*n*]CPPDs (n = 2 to 8) are shown in Fig. 8. The $\Delta_f H^\circ_{298}$ per-unit monomer of all *cis* isomer is higher than that of all *trans* isomers indicating the higher strain and less stable compared to *trans* isomers. The $\Delta_f H^\circ_{298}$ per-unit monomer of *cis* isomer reaches to the plateau for n = 7 and 8. However, for the *trans* isomer $\Delta_f H^\circ_{298}$ per-unit monomer decreases linearly. We have also calculated energy difference between $\Delta_f H^\circ_{298}/n$ – SE/n for [*n*]CPPDs (Table 2). The average $\Delta_f H^\circ_{298}/n$ – SE/n value for all *cis* and all *trans*-[*n*]CPPDs is ~330 kJ mol^{-1}. This value is very close to $\Delta_f H^\circ_{298}$ of strain free Ph–N=N–H (334 kJ mol^{-1}).

Table 2 also contains the enthalpies of combustion ($\Delta_{comb} H^\circ_{298}$) and molar enthalpy of combustion. It can be seen that absolute value for CPPDs is ~–(30–32) kJ g^{-1} indicating the release a large amount of energy during the combustion of CPPDs. Moreover, the replacement of N=N bond by C≡C bond

Table 2 $\Delta_f H^\circ_{298}$ (kJ mol^{-1}), $\Delta_f H^\circ_{298}/n$ – SE/n (kJ mol^{-1}) and enthalpies of combustion (kJ mol^{-1}) for [*n*]CPPDs (n = 2 to 8)

[*n*]CPPDs	$\Delta_f H^\circ_{298}$	$\Delta_f H^\circ_{298}/n$ – SE/n	$\Delta_{comb} H^\circ_{298}$ [a]	$\Delta_{comb} H^\circ_{298}$ [b]
[2$_c$]CPPD	1009	328.8	−6698.1	−32.2
[2$_t$]CPPD	1059.1	328.7	−7722.6	−37.1
[3$_c$]CPPD	1214.3	329.6	−9747.9	−31.2
[3$_t$]CPPD	1283.1	320.1	−10794.6	−34.6
[4$_c$]CPPD	1564.1	329.6	−12942.2	−31.1
[4$_t$]CPPD	1652.5	329.4	−13044.8	−31.3
[5$_c$]CPPD	1972.2	329.8	−16194.7	−31.1
[5$_t$]CPPD	1904.0	329.7	−16144.3	−31.0
[6$_c$]CPPD$_1$	2368.4	329.9	−19435.5	−31.1
[6$_c$]CPPD$_2$	2356.4	329.9	−19423.4	−31.1
[6$_t$]CPPD	2185.9	329.9	−19274.3	−30.8
[7$_c$]CPPD$_1$	2704.2	330.0	−22615.7	−31.1
[7$_c$]CPPD$_2$	2715.9	330.1	−22627.4	−31.1
[7$_t$]CPPD	2471.8	330.0	−22408.3	−30.7
[8$_c$]CPPD$_1$	3086.3	330.1	−25842.4	−31.0
[8$_c$]CPPD$_2$	3085.2	330.0	−25841.3	−31.0
[8$_t$]CPPD	2751.6	330.2	−25562.1	−30.6

[a] A generalised combustion reaction of [*n*]CPPDs: [*n*]CPPDs + 7nO$_2$ → 6nCO$_2$ + 2nH$_2$O + nN$_2$. [b] Molar enthalpy of combustion (in kJ g^{-1}).

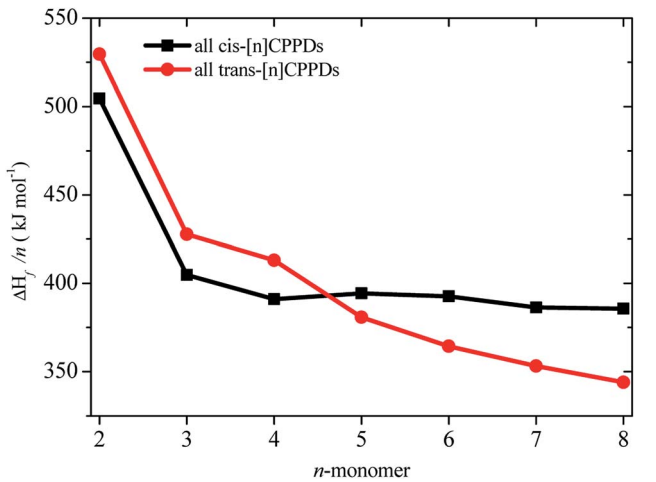

Fig. 8 $\Delta_f H^\circ_{298}$ per-unit monomer of all *cis* and all *trans* isomers of [*n*] CPPDs (n = 2 to 8).

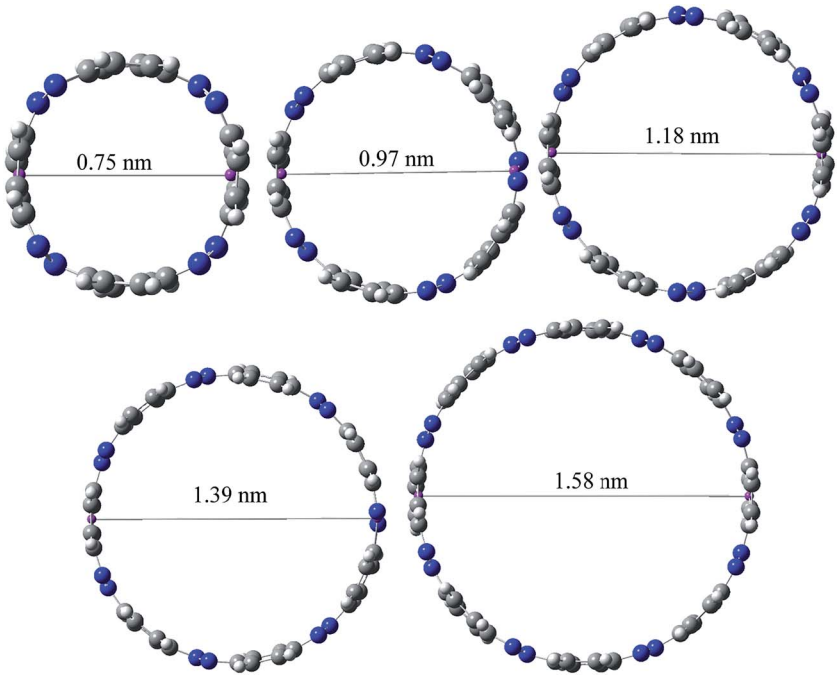

Fig. 9 Ring diameters for *trans*-[n_t]CPPDs (n = 4 to 8).

in CPPDs results in increasing the C atoms, leading to a relatively higher absolute value of $\Delta_{comb}H^{\circ}_{298}$ for CPPAs. This indicates that C atoms contribute ~8–9 kJ g^{-1} energy through the formation of carbon dioxide during combustion, which can explain the higher $\Delta_{comb}H^{\circ}_{298}$ of CPPAs than that of CPPDs.

3.3 Electronic properties of [*n*]CPPDs

Ring diameter is good indicator of host–guest chemistry[26] of [*n*]CPPDs and it is estimated as the distance between the centres of mass of the opposite benzene ring for the even member of all *trans* CPPDs *i.e.*, [4$_t$]CPPD, [6$_t$]CPPD, and [8$_t$]CPPD and the distance between the nitrogen atom and the center of mass of the opposite benzene ring for the odd number of *trans* CPPDs *i.e.*, [5$_t$]CPPD and [7$_t$]CPPD (see Fig. 9). As expected, when azo groups are all in *trans* configuration, the nanorings are in open state in which the cavities are available and when the azo groups are all in *cis* forms, they are in the closed state in which the cavities are deformed or collapsed. The cavity diameter (D_n) from [4$_t$]CPPD to [8$_t$]CPPD evolves linearly with increasing phenylenediazene units (n); for example, the B3LY/6-31+G(d,p) results can be described by equation (the regression coefficient is 0.99968)

$$D_n\ (\text{nm}) = -0.074 + n \times 0.208.$$

The trend of ring diameters is similar to SE of [n_t]CPPDs (n = 4 to 8). When the size of the system increases, SE decreasing with increasing the ring diameter. The calculated ring diameter of [6$_t$]CPPDs (1.18 nm) and [7$_t$]CPPDs (1.39 nm) are also in very good agreement with the values reported by Yuan *et al.*[26] for [6$_t$]CPPD (1.19 nm) and [7$_t$]CPPD (~1.39 nm) calculated using M06-2X/6-31G(d) level of theory. Moreover, comparing the diameter of [n_t]CPPDs (n = 4 to 8) with their analogous [n]CPPAs (n = 4 to 8) and [n]CPPs (n = 4 to 8) nanorings (ESI Table S7†). The values of [n_t]CPPDs (n = 4 to 8) are lower than those of corresponding [n]CPPAs and [n]CPPs.

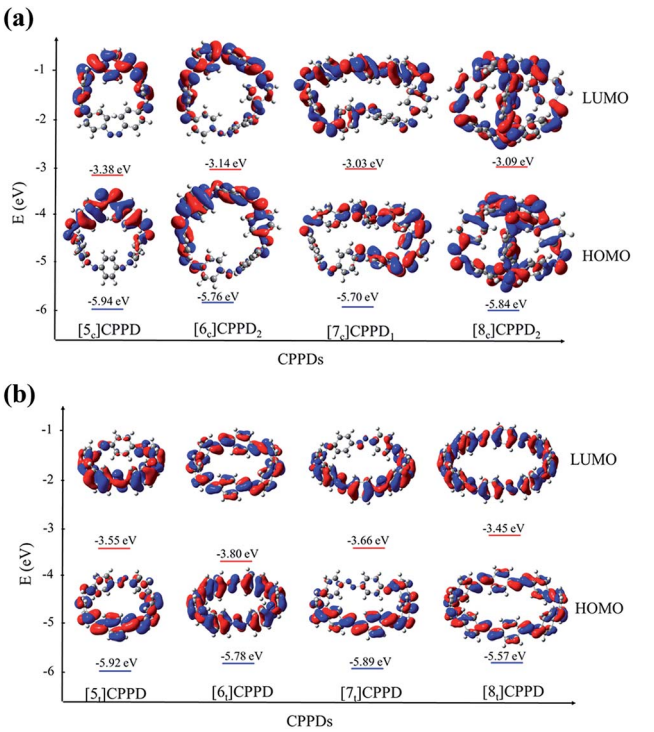

Fig. 10 (a) Spatial distribution (0.02 au) and energy level diagram of HOMO and LUMO orbitals for *cis* isomer of [*n*]CPPD (n = 5 to 8). (b) Spatial distribution (0.02 au) and energy level diagram of HOMO and LUMO orbitals for *trans* isomers of [*n*]CPPDs (n = 5 to 8).

The cavity size of [6_t]CPPD (1.18 nm) is almost comparable to that of (1.01 nm) carbon nanotube, and it appears to be suitable for the inclusion of C_{60} (0.7 nm in diameter). In the previous study, Zhao and Truhlar[56] have calculated the interaction energies of guest molecules such as three arm-chair-type nanotubes; (3, 3), (4, 4), and (5, 5) with the host molecules such as [6]CPPA, (3,3) [6]CPPA, (4,4) [6]CPPA, and (5,5) [6]CPPA using the density functional theory. In another study, Bachrach and Zayat[57] have calculated binding free energies of host [14] CPP and guest molecule [*n*]CPP (*n* = 6 to 10), [14]CPP [6]CPP, [14]CPP [7]CPP, [14]CPP [7]CPP, [14]CPP [8]CPP, [14]CPP [9]CPP, and [14]CPP [10]CPP using ωB97X-D/6-31G(d) level calculation. In 2015, Yuan *et al.*[26] have predicted the host–guest interaction between [6]CPPD nanoring with C_{60}. Recently, Lee *et al.*[58] have synthesized [3]CPP C_{70} and [3]CPPA C_{70} and calculated cavity diameter using B3LYP/6-31G(d) level of theory. A similar

Table 3 Comparison of structural properties and SE of CPPDs with carbon nanoring models

Properties	[6]CPP[23]	[6]CPPA[22]	[6]CPPD
	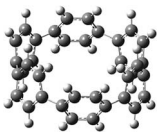	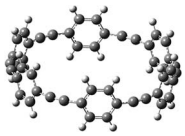	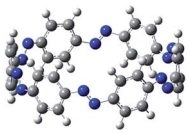
Angle (degree)	12.6	165.3	158.8
C–C bond (Å)	1.490	1.421	1.413 (C–N)
Point group	D_{3h}	D_{6h}	D_6
SE (kJ mol^{-1})	406.8	164.4	206.4
Diameter (nm)	0.79	1.30	1.18
H–L (eV)	3.14	3.02	1.98
Experimental study	Synthesized[23]	Synthesized[22]	*Synthesis required*
	[7]CPP[23]	[7]CPPA[22]	[7]CPPD
	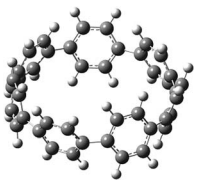	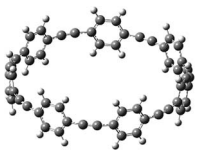	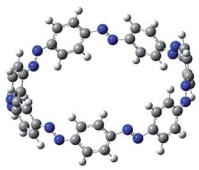
Angle (degree)	10.9	167.6	160.6
C–C bond (Å)	1.487	1.420	1.410 (C–N)
Point group	C_2	D_{7h}	D_7
SE (kJ mol^{-1})	356.5	133.3	161.8
Diameter (nm)	0.95	1.53	1.39
H–L (eV)	2.22	3.32	3.17
Experimental study	Synthesized[23]	Synthesized[22]	*Synthesis required*
	[8]CPP[23]	[8]CPPA[22]	[8]CPPD
	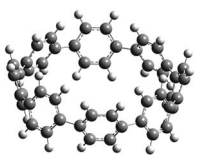	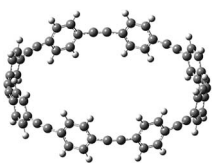	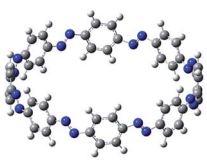
Angle (degree)	9.3	169.3	164.1
C–C bond (Å)	1.487	1.419	1.413(C–N)
Point group	D_{4h}	D_{8h}	D_8
SE (kJ mol^{-1})	307.1	109.4	110
Diameter (nm)	1.1	1.73	1.58
H–L (eV)	2.12	3.05	3.14
Experimental study	Synthesized[23]	Synthesized[22]	*Synthesis required*

approach can be applied to design host–guest systems with host CPPDs and guest molecules such as C_{60}, C_{70}, (3,3), (4,4) and (5,5), CPPs, and CPPAs to understand the chemical and electronic properties.

Molecular orbital is an important parameter, which can provide useful information on the electronic structure and a decisive factor indicating potential material for the construction of solar cells. The calculated highest occupied molecular orbitals (HOMO) and lowest unoccupied molecular orbitals (LUMO) are provided in ESI Table S7† and their spatial distribution are shown in Fig. 10. The HOMO and LUMO of [6_c]CPPD$_1$, [6_t]CPPD, and [8_t]CPPD show the uniform orbital density located at all atoms in the skeleton, whereas the HOMO and LUMO of [5_c]CPPD, [6_c]CPPD$_2$, [5_t]CPPD, and [7_c]CPPD$_1$, [7_t]CPPD have non-uniform orbital density on Ph–N=N unit. The HOMO and LUMO levels of [5_t]CPPD and [7_t]CPPD are 2-fold degenerate, which indicate that the removal of an electron from the HOMO level or addition of an electron to the LUMO level could weaken the skeleton framework.[59] The values of HOMOs and LUMOs of the odd *trans*-CPPDs are higher than that of even *trans*-CPPDs. However, the odd-even trend was not observed in *cis*-CPPDs. This is probably due to conformational differences of the odd and even CPPDs as described above. The spatial distribution of HOMO–LUMO gap for CPPDs were also compared with CPPs and CPPAs. As for CPPDs, the HOMO and LUMO distribution are quite different from CPPAs and CPPs.

Table S7† also includes the HOMO–LUMO gap values for CPPAs and CPPs. The HOMO–LUMO gap of CPPDs is in between 1.98 and 2.85 eV, for CPPAs (2.99 to 3.05 eV) and for CPPs (2.55–3.41 eV). The predicted HOMO–LUMO gap of all *cis*-CPPDs and all *trans* CPPDs have smaller values than that of CPPAs and CPPs. Our calculations also suggest that adding nitrogen atoms in CPPs decreases the HOMO–LUMO gap, which is in consistent with the data reported by Van Raden *et al.*,[27] who have also predicted the decreasing value of HOMO–LUMO gap of nitrogen doped CPP *i.e.*, azo[6]CPP. The predicted HOMO–LUMO gap of CPPDs are in the range of the material used in the construction of solar cells. The results suggest that CPPDs oligomer are better candidate for building solar cells than CPPAs and CPPs.

3.4 Comparison of CPPDs with carbon nanorings (CNRs)

The structure, electronic properties, and thermochemistry of all *trans*-[*n*]CPPDs (n = 6 to 8) were compared with its analogous carbon nanoring structure *i.e.*, [*n*]CPPs and [*n*]CPPAs (n = 6 to 8) are given in Table 3. Results indicate that nitrogen substituted cyclic *para* phenyl oligomer have higher strain energies compared to acetylene substituted cyclic paraphenyl oligomer. However, strain energies of CPPs are higher than the strain energies of CPPAs and CPPDs. The ring diameter of all three species are also correlated with molecular strain. The lower value of diameter of nanoring has higher strain energies and higher value of diameter has lower strain energies. The HOMO–LUMO gap of these nanorings suggests that CPPDs could be the good material for the construction of solar cells. In addition, it may be possible to design host–guest systems with hosts; [6]CPPD, [7]CPPD, and [8]CPPD with guest molecules; C_{60}, C_{70}, CPPs (3,3), (4,4) and (5,5), CPPAs and carbon nanotubes to understand their chemistry. The predicted structure, SE, and electronic properties of CPPDs with carbon nanoring structure (CPAs and CPPAs) (Table 3), suggest that [6_t]CPPD, [7_t]CPPD, and [8_t]CPPD can be synthesized in the laboratory.

4. Conclusions

We have provided the theoretical calculation related to the structure, strain energies (SE), standard enthalpies of formation ($\Delta_f H^\circ_{298}$), and electronic properties of the novel structures of all *cis* and all *trans* isomers of [*n*]CPPDs (n = 2 to 8). The calculations of SE and $\Delta_f H^\circ_{298}$ are based on homodesmotic reaction approach and B3LYP hybrid DFT method with 6-31+G(d,p) basis set. The SE and ring diameter of CPPDs indicate [6_t]CPPD, [7_t]CPPD, and [8_t]CPPD are the ideal molecules for the future experimental study. The unique behaviour of HOMO and LUMO of CPPDs compared to CPPAs and CPPs opens a new possibility of CPPDs for applications in optoelectronics. The trends observed for ring systems presented here are not just limited to CPPDs but rather applicable to a wide range of photo convertible molecules. Our campaign toward the design of mix combination of CPPDs is underway and will be reported in future. We believe that the ring effect uncovered in this study may find uses in the emerging field of organic electronics. The present study should help us not only to plan a new synthetic strategy but also to understand the structural, electronic, physical properties, and the host-guest chemistry of other nitrogen doped cyclic oligomer.

Conflicts of interest

There are no conflicts to declare.

Acknowledgements

Author gratefully acknowledge the computational resources at KISTI super computer facility in the South Korea. MAA thanks Sejong University Seoul for the research support. MAA thanks Professor John R. Barker from University of Michigan for useful suggestions. We thank the anonymous reviewers for helpful suggestions, including the suggestion to find out other conformations of *cis* and *trans*-CPPDs. M. A. Alam thanks, ABI-A-State (Grant number: Start-up 200127) for supporting.

References

1 C. Pu, D. Zhou, Y. Li, H. Liu, Z. Chen, Y. Wang and Y. Ma, *J. Phys. Chem. C*, 2017, **121**, 2669–2674.
2 Y. Liu, A. Singharoy, C. G. Mayne, A. Sengupta, K. Raghavachari, K. Schulten and A. H. Flood, *J. Am. Chem. Soc.*, 2016, **138**, 4843–4851.
3 X. Wang, X. Li, L. Zhang, Y. Yoon, P. K. Weber, H. Wang, J. Guo and H. Dai, *Science*, 2009, **324**, 768–771.
4 T. Cui, R. Lv, Z.-H. Huang, H. Zhu, J. Zhang, Z. Li, Y. Jia, F. Kang, K. Wang and D. Wu, *Carbon*, 2011, **49**, 5022–5028.

5 L. Qu, Y. Liu, J. B. Baek and L. Dai, *ACS Nano*, 2010, **4**, 1321–1326.
6 A. L. M. Reddy, A. Srivastava, S. R. Gowda, H. Gullapalli, M. Dubey and P. M. Ajayan, *ACS Nano*, 2010, **4**, 6337–6342.
7 W. R. Browne and B. L. Feringa, *Nat. Nanotechnol.*, 2006, **1**, 25–35.
8 T. Hugel, N. B. Holland, A. Cattani, L. Moroder, M. Seitz and H. E. Gaub, *Science*, 2002, **296**, 1103–1106.
9 H. M. Jeong, J. W. Lee, W. H. Shin, Y. J. Choi, H. J. Shin, J. K. Kang and J. W. Choi, *Nano Lett.*, 2011, **11**, 2472–2477.
10 A. Khan, C. Kaiser and S. Hecht, *Angew. Chem., Int. Ed.*, 2006, **45**, 1878–1881.
11 K. K. Cotí, M. E. Belowich, M. Liong, M. W. Ambrogio, Y. A. Lau, H. A. Khatib, J. I. Zink, N. M. Khashab and J. F. Stoddart, *Nanoscale*, 2009, **1**, 16–39.
12 Y. Yang, R. P. Hughes and I. Aprahamian, *J. Am. Chem. Soc.*, 2014, **136**, 13190–13193.
13 W. A. Velema, W. Szymanski and B. L. Feringa, *J. Am. Chem. Soc.*, 2014, **136**, 2178–2191.
14 D. Hoersch, S.-H. Roh, W. Chiu and T. Kortemme, *Nat. Nanotechnol.*, 2013, **8**, 928–932.
15 J. E. Koskela, V. Liljeström, J. Lim, E. E. Simanek and R. H. Ras, *J. Am. Chem. Soc.*, 2014, **136**, 6850–6853.
16 Y. Norikane, K. Kitamoto and N. Tamaoki, *J. Org. Chem.*, 2003, **68**, 8291–8304.
17 S. A. Nagamani, Y. Norikane and N. Tamaoki, *J. Org. Chem.*, 2005, **70**, 9304–9313.
18 H. Rau and E. Lueddecke, *J. Am. Chem. Soc.*, 1982, **104**, 1616–1620.
19 E. Durgun and J. C. Grossman, *J. Phys. Chem. Lett.*, 2013, **4**, 854–860.
20 J. Olmsted III, J. Lawrence and G. G. Yee, *Sol. Energy*, 1983, **30**, 271–274.
21 M. A. Ali and M. S. Krishnan, *Mol. Phys.*, 2009, **107**, 2149–2158.
22 T. Kawase and H. Kurata, *Chem. Rev.*, 2006, **106**, 5250–5273.
23 E. R. Darzi and R. Jasti, *Chem. Soc. Rev.*, 2015, **44**, 6401–6410.
24 Y. Segawa, H. Omachi and K. Itami, *Org. Lett.*, 2010, **12**, 2262–2266.
25 S. E. Lewis, *Chem. Soc. Rev.*, 2015, **44**, 2221–2304.
26 K. Yuan, J.-S. Dang, Y.-J. Guo and X. Zhao, *J. Comput. Chem.*, 2015, **36**, 518–528.
27 J. M. Van Raden, E. R. Darzi, L. N. Zakharov and R. Jasti, *Org. Biomol. Chem.*, 2016, **14**, 5721–5727.
28 A. von Baeyer, *Ber. Dtsch. Chem. Ges.*, 1885, **18**, 2278.
29 F. Klappenberger, Y.-Q. Zhang, J. Bjork, S. Klyatskaya, M. Ruben and J. V. Barth, *Acc. Chem. Res.*, 2015, **48**, 2140–2150.
30 F. H. Westheimer, *Special Publication No. 8*, The Chemical Society, London, 1957, p. 1.
31 T. Dudev and C. Lim, *J. Am. Chem. Soc.*, 1998, **120**, 4450–4458.
32 W. J. Hehre, R. Ditchfield, L. Radom and J. A. Pople, *J. Am. Chem. Soc.*, 1970, **92**, 4796–4801.
33 O. V. Dorofeeva and O. N. Ryzhova, *J. Phys. Chem. A*, 2016, **120**, 2471–2479.
34 P. Wessig, M. Czarnecki, D. Badetko, U. Schilde and A. Kelling, *J. Org. Chem.*, 2016, **81**, 9147–9157.
35 R. V. Williams, A. G. Al-Sehemi, A. K. Meier, Z. Z. Brown and J. R. Armantrout, *J. Org. Chem.*, 2017, **82**, 4136–4147.
36 R. Notario, M. V. Roux and O. Castano, *Phys. Chem. Chem. Phys.*, 2011, **3**, 3717–3721.
37 N. Sebbar, H. Bockhorn and J. W. Bozzelli, *Phys. Chem. Chem. Phys.*, 2002, **4**, 3691–3703.
38 R. O. Ramabhadran and K. Raghavachari, *Acc. Chem. Res.*, 2014, **47**, 3596–3604.
39 S. E. Wheeler, K. N. Houk, P. R. Schleyer and W. D. Allen, *J. Am. Chem. Soc.*, 2009, **131**, 2547–2560.
40 M. A. Ali and M. S. Krishnan, *J. Org. Chem.*, 2010, **75**, 5797–5809.
41 P. Nava and Y. Carissan, *Phys. Chem. Chem. Phys.*, 2014, **16**, 16196–16203.
42 A. D. Becke, *J. Chem. Phys.*, 1993, **98**, 5648–5652.
43 M. J. Frisch, G. W. Trucks, H. B. Schlegel, G. E. Scuseria, M. A. Robb, J. R. Cheeseman, G. Scalmani, V. Barone, B. Mennucci and G. A. Petersson, *Gaussian 09, Revision D.01*, Gaussian, Inc., Wallingford CT, 2009.
44 M. J. Frisch, G. W. Trucks, H. B. Schlegel, G. E. Scuseria, M. A. Robb, J. R. Cheeseman, G. Scalmani, V. Barone, B. Mennucci and G. A. Petersson, *Gaussian 09, Revision E.01*, Gaussian, Inc., Wallingford CT, 2009.
45 M. Moral, A. Pérez-Guardiola, E. San-Fabián, A. J. Pérez-Jiménez and J. C. Sancho-García, *J. Phys. Chem. C*, 2016, **120**, 22069–22078.
46 M. R. Golder, C. E. Colwell, B. M. Wong, L. N. Zakharov, J. Zhen and R. Jasti, *J. Am. Chem. Soc.*, 2016, **138**, 6577–6582.
47 D. Vijay, E. Varathan and V. Subramanian, *J. Mater. Chem. A*, 2013, **1**, 4358–4369.
48 M. A. Ali and S. Sen, *Thermochim. Acta*, 2017, **654**, 146–156.
49 L. A. Curtiss, P. C. Redfern and K. Raghavachari, *J. Chem. Phys.*, 2007, **126**, 084108.
50 J. A. Bouwstra, A. Schouten and J. Kroon, *Acta Crystallogr., Sect. C: Cryst. Struct. Commun.*, 1983, **39**, 1121–1123.
51 Y. Segawa, A. Fukazawa, S. Matsuura, H. Omachi, S. Yamaguchi, S. Irle and K. Itami, *Org. Biomol. Chem.*, 2012, **10**, 5979–5984.
52 T. Iwamoto, Y. Watanabe, Y. Sakamoto, T. Suzuki and S. Yamago, *J. Am. Chem. Soc.*, 2011, **133**, 8354–8361.
53 E. Kayahara, V. K. Patel and S. Yamago, *J. Am. Chem. Soc.*, 2014, **136**, 2284–2287.
54 H. Y. Afeefy, J. F. Liebman and S. E. Stein, MD, 2017, http://webbook.nist.gov, retrieved 03.28.2017.
55 M. H. Matus, A. J. Arduengo III and D. A. Dixon, *J. Phys. Chem. A*, 2006, **110**, 10116–10121.
56 Y. Zhao and D. G. Truhlar, *J. Am. Chem. Soc.*, 2007, **129**, 8440–8442.
57 S. M. Bachrach and Z. C. Zayat, *J. Org. Chem.*, 2016, **81**, 4559–4565.
58 S. Lee, E. Chénard, D. L. Gray and J. S. Moore, *J. Am. Chem. Soc.*, 2016, **138**, 13814–13817.
59 C. Shen, P. Wang and M. Lu, *J. Phys. Chem. A*, 2015, **119**, 8250–8255.